BIOCHEMISTRY
including biophysical chemistry & molecular biology

Article

pubs.acs.org/biochemistry

Redesign of Substrate Specificity and Identification of the Aminoglycoside Binding Residues of Eis from *Mycobacterium tuberculosis*

Benjamin C. Jennings,[†,§] Kristin J. Labby,[†,§] Keith D. Green,[‡] and Sylvie Garneau-Tsodikova*[,‡]

[†]Life Sciences Institute, 210 Washtenaw Avenue, University of Michigan, Ann Arbor, Michigan 48109-2216, United States
[‡]Department of Pharmaceutical Sciences, University of Kentucky, Lexington, Kentucky 40536-0596, United States

Supporting Information

ABSTRACT: The upsurge in drug-resistant tuberculosis (TB) is an emerging global problem. The increased expression of the enhanced intracellular survival (Eis) protein is responsible for the clinical resistance to aminoglycoside (AG) antibiotics of *Mycobacterium tuberculosis*. Eis from *M. tuberculosis* (Eis_*Mtb*) and *M. smegmatis* (Eis_*Msm*) function as acetyltransferases capable of acetylating multiple amines of many AGs; however, these Eis homologues differ in AG substrate preference and in the number of acetylated amine groups per AG. The AG binding cavity of Eis_*Mtb* is divided into two narrow channels, whereas Eis_*Msm* contains one large cavity. Five bulky residues lining one of the AG binding channels of Eis_*Mtb*, His119, Ile268, Trp289, Gln291, and Glu401, have significantly smaller counterparts in Eis_*Msm*, Thr119, Gly266, Ala287, Ala289, and Gly401, respectively. To identify the residue(s) responsible for AG binding in Eis_*Mtb* and for the functional differences from Eis_*Msm*, we have generated single, double, triple, quadruple, and quintuple mutants of these residues in Eis_*Mtb* by mutating them into their Eis_*Msm* counterparts, and we tested their acetylation activity with three structurally diverse AGs: kanamycin A (KAN), paromomyin (PAR), and apramycin (APR). We show that penultimate C-terminal residue Glu401 plays a critical role in the overall activity of Eis_*Mtb*. We also demonstrate that the identities of residues Ile268, Trp289, and Gln291 (in Eis_*Mtb* nomenclature) dictate the differences between the acetylation efficiencies of Eis_*Mtb* and Eis_*Msm* for KAN and PAR. Finally, we show that the mutation of Trp289 in Eis_*Mtb* into Ala plays a role in APR acetylation.

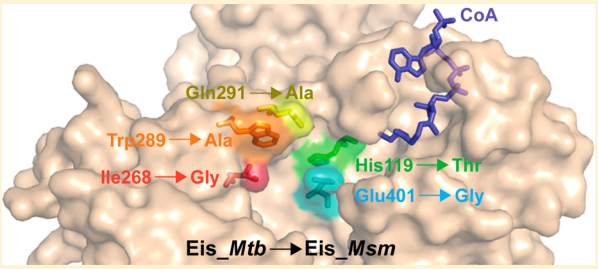

Aminoglycosides (AGs) (Figure 1A) are broad-spectrum antibiotics used to treat many serious bacterial infections including multidrug-resistant (MDR) and extensively drug-resistant (XDR) tuberculosis (TB). Resistance to AGs is increasing, leading to a higher number of cases of extremely and totally drug-resistant TB.[1−3] In *Mycobacterium tuberculosis* (*Mtb*), upregulation of the enhanced intracellular survival (*eis*) gene is responsible for its resistance to the second-line anti-TB drugs kanamycin A (KAN, Figure 1A) and amikacin.[4−6] The Eis protein is an acetyltransferase that efficiently acetylates AGs, thereby inactivating them as antibiotics.[4,7]

Mtb and the homologous nonpathogenic model mycobacterium *M. smegmatis* (*Msm*) share many (>2000) protein homologues, including virulence genes, and they maintain the same unusual cell-wall structure.[8] We previously reported that Eis from *Mtb* (Eis_*Mtb*) and *Msm* (Eis_*Msm*) are acetyl coenzyme A (AcCoA)-dependent acetyltransferases capable of multiacetylating a variety of AGs[7,9] and lysine-containing peptides such as the anti-TB drug capreomycin.[10] However, the actual number of acetylations and the positions of the amines that get acetylated are highly dependent on the structure of the AG being modified (Figure 1B). Despite their high sequence (Figure 2) and structural (Figure 3A) similarities, Eis_*Mtb* and Eis_*Msm* differ in their substrate and inhibition profiles. One difference is that Eis_*Msm* is capable of diacetylating the rigid fused-ring AG apramycin (APR, Figure 1A), whereas APR is a poorer substrate for Eis_*Mtb*.[9]

A structural examination of these two Eis homologues revealed striking differences in their AG binding pockets. The substrate binding pocket of Eis_*Mtb* is divided by Glu401 into two narrow channels (Figure 3C).[7] In contrast, because the corresponding residue in Eis_*Msm* is the much smaller Gly401, the binding pocket of Eis_*Msm* is one large, continuous cavity (Figure 3D).[11] Residues lining the AG binding pocket in Eis_*Mtb* include Ile268, Trp289, Gln291, and Glu401 (Figure 2). In Eis_*Msm*, these residues correspond to Gly266, Ala287, Ala289, and Gly401, respectively, which are all much smaller than those in Eis_*Mtb*. We previously proposed that the larger size of the AG binding cavity of Eis_*Msm* helps APR acetylation.[9] In addition, His119 (Thr119 in Eis_*Msm*), which is located in the binding pocket, was previously demonstrated to be important for the acetylation activity of

Received: March 7, 2013
Revised: June 10, 2013
Published: July 9, 2013

   dx.doi.org/10.1021/bi4002985 | *Biochemistry* 2013, 52, 5125−5132

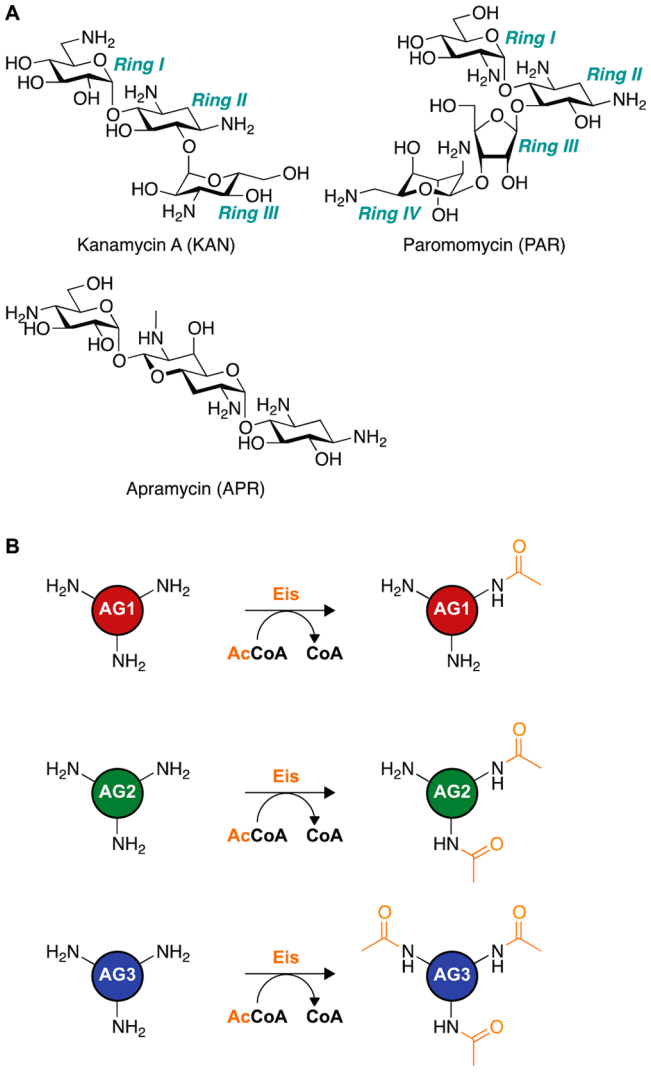

Figure 1. (A) Structures of the AGs used in this study: kanamycin A (KAN), paromomycin (PAR), and apramycin (APR). (B) Schematic of the reaction catalyzed by Eis enzymes. Eis is capable of mono-, di-, or triacetylating AGs, depending on the AG structure and the Eis isoform. To date, the positions of acetylation (1, 2′, and 6′) by Eis_*Mtb* have been reported only for neamine.[7]

Eis.[7] As observed in the previously published crystal structure of Eis_*Mtb*, the position of the backbone of His119 must be critical for catalysis because its backbone amide coordinates the catalytic water molecule to the amino group of the AG, positioning it for acetylation. We previously demonstrated that mutation of His119 to Ala reduced Eis_*Mtb* activity with 10 different AGs, suggesting that the side chain of His119 also plays an important role in AG binding or catalysis.[7]

To investigate the role of these five residues in AG binding, we have conducted a mutational analysis by redesigning the Eis_*Mtb* active site to contain residues from Eis_*Msm*. Single mutations (H119T, I268G, W289A, Q291A, and E401G) of the residues lining the AG binding pocket were generated to explore their individual roles in AG binding and enzymatic activity. These mutations were also combined to form additional double, triple, quadruple, and quintuple Eis_*Mtb* mutants to investigate the overall flexibility of the AG binding pocket. The initial activity profiles of the purified Eis_*Mtb* mutants were determined with three AGs: KAN, paromomycin (PAR), and APR. The mutant−AG pairs displaying reasonable activity were further characterized to determine their Michaelis−Menten kinetic constants. Interpreting these results within the context of the Eis structure reveals important properties governing AG binding to Eis.

MATERIALS AND METHODS

Bacterial Strains, Plasmids, Materials, and Instrumentation. All chemicals, including 5,5′-dithio-(2-nitrobenzoic acid) (DTNB), AcCoA, APR, and KAN were purchased from Sigma-Aldrich (Milwaukee, WI), with the exception of PAR, which was purchased from AK Scientific (Mountain View, CA). The pH of the buffers was adjusted at rt. Chemically competent *Escherichia coli* TOP10 and BL21(DE3) strains were purchased from Invitrogen (Carlsbad, CA). The pET28a plasmid used for cloning experiments was purchased from Novagen (Gibbstown, NJ). PCR primers were purchased from Integrated DNA Technologies (Coralville, IA). Restriction enzymes, Phusion DNA polymerase, T4 DNA ligase, and all other cloning reagents were purchased from New England Biolabs (Ipswich, MA). Spectrophotometric assays were performed in 96-well plates using a multimode SpectraMax M5 plate reader from Molecular Devices (Sunnyvale, CA). Liquid chromatography mass spectrometry (LCMS) was performed with a Shimadzu LCMS-2019EV composed of an LC-20AD liquid chromatograph and an SPD-20AV UV−vis detector. The PDB structures 3R1K (Eis_*Mtb*)[7] and 3SXN (Eis_*Msm*)[11] were visualized using PyMOL (The PyMOL Molecular Graphics System, version 1.5.0.4, Schrödinger, LLC).

Preparation of Eis_*Mtb* Mutant Constructs by Site-Directed Mutagenesis. The splicing by overlap extension (SOE) method[12] was used to create all single (H119T, I268G, W289A, Q291A, and E401G mutants, which are abbreviated as H, I, W, Q, and E, respectively), double (HI, HE, IW, IE, WQ, and WE), triple (HIW, HIE, HWQ, IWQ, and WQE), quadruple (HIWE and HWQE), and quintuple (HIWQE) Eis_*Mtb* mutant constructs. The primers used for the amplification of the *eis_Mtb* mutant gene sequences are listed in Tables S1 and S2 of the Supporting Information. The H, I, W, Q, and E single mutants and the WQ double mutant were first constructed using pEis_*Mtb*-pET28a that we previously generated[7] as the template. In the first round of PCR, the gene fragments upstream and downstream of the mutation(s) were individually amplified in two separate reactions: (1) using the 5′ primer for *eis_Mtb*-wt with the 3′ primer for the mutant and (2) using the 5′ primer for the *mutant* with the 3′ primer for *eis_Mtb*-wt, respectively (Table S1). After gel purification, the resulting pairs of PCR fragments were combined and used as templates for the second round of PCR amplification using the 5′ and 3′ primers for *eis_Mtb*-wt (Table S1). A pET28a vector, linearized at the *Nde*I and *Bam*HI restriction sites, was used for the insertion of the digested mutant complete PCR products to generate the plasmids used for overexpression and protein purification. The double, triple, quadruple, and quintuple mutants were constructed similarly using the single, double, triple, and quadruple mutants as templates, respectively. The construction of all 19 mutants is summarized in Table S2 of the Supporting Information. The Eis_*Mtb* mutant-containing plasmids were transformed into TOP10 *E. coli* cells. The *eis_Mtb* mutant sequences were confirmed by DNA sequencing (University of Michigan DNA Sequencing Core) and comparison to the *eis_Mtb*-wt sequence (TB Database gene locus Rv2416c).

dx.doi.org/10.1021/bi4002985 | *Biochemistry* 2013, 52, 5125−5132

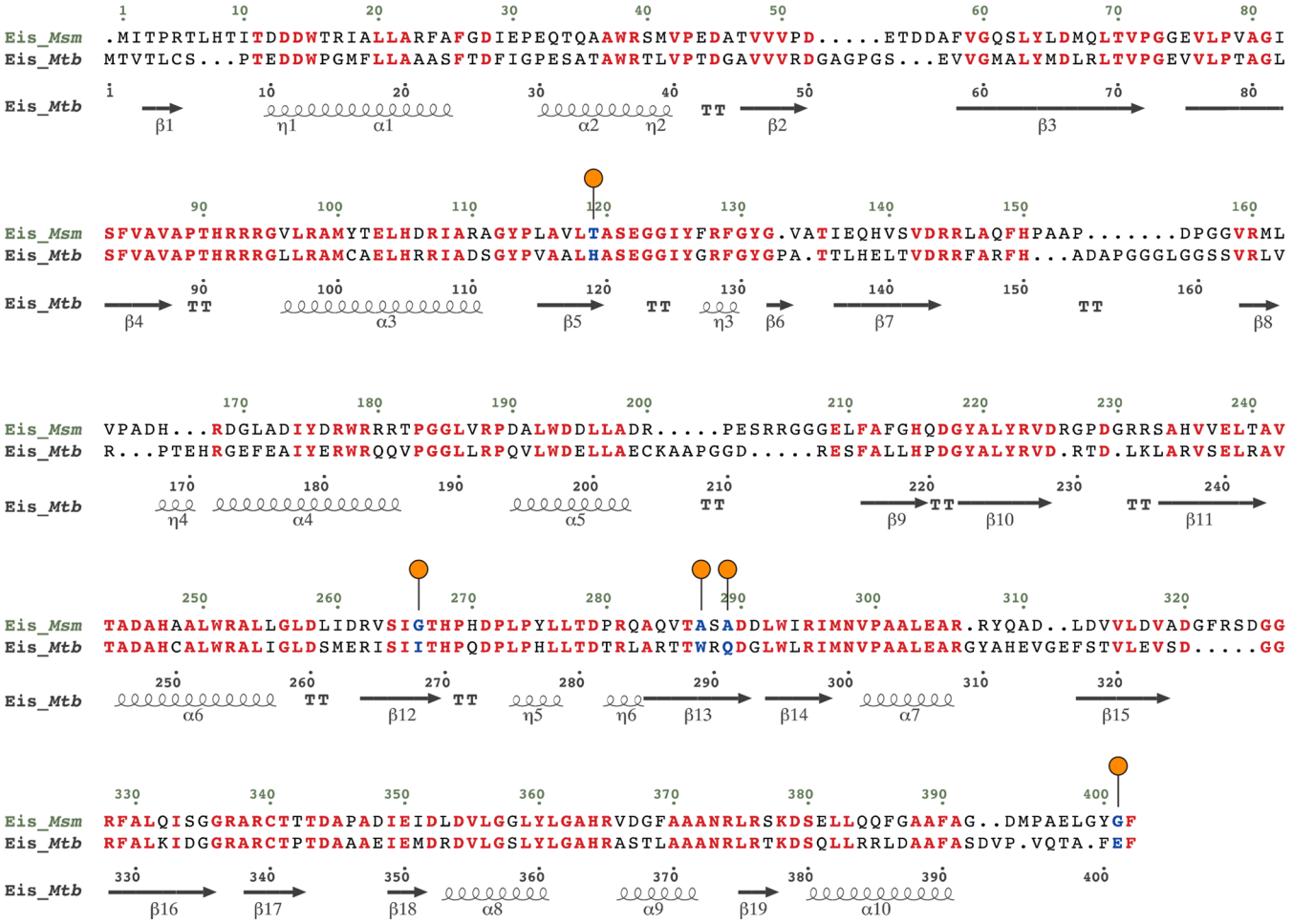

Figure 2. Structure-based sequence alignment of Eis_*Mtb* and Eis_*Msm*. Residues in red are conserved between the two Eis homologues. Residues mutated in this study are blue and are marked with orange circles above the sequence. α, β, η, and T represent α-helix, β-sheet, 3_{10}-helix, and β-turn, respectively

Overexpression and Purification of Eis_*Mtb* Mutants. Eis_*Mtb* mutants containing an N-terminal His_6 tag were overexpressed in *E. coli* BL21(DE3) and purified by using Ni^{II}-NTA agarose resin (Qiagen) following the procedures that we previously described for Eis_*Mtb*[7] and Eis_*Msm*.[9] The fractions containing the desired Eis_*Mtb* mutant proteins, determined by SDS-PAGE, were pooled, dialyzed into Tris-HCl (50 mM, pH 8.0) overnight, and stored at 4 °C where they retained activity for at least 1 month. The yields of the purified Eis_*Mtb*, Eis_*Msm*, and Eis_*Mtb* mutants (Table S3) and their purities (Figure S1) are reported in the Supporting Information.

Determination of Eis_*Mtb* Mutant Activity with KAN, PAR, and APR by Spectrophotometric Assay. Ellman's reagent was used to determine the acetyltransferase activity of all 19 Eis_*Mtb* mutants with KAN, PAR, and APR. Briefly, the thiol group of the released CoA reacted with DTNB, and the increase in absorbance (ε_{412} = 14 150 M^{-1} cm^{-1})[13] was monitored at 412 nm. The addition of Eis_*Mtb* mutant (0.5 μM) initiated the reactions (200 μL) containing AGs (APR, KAN, or PAR, 0.1 mM, 1 equiv), AcCoA (0.5 mM, 5 equiv), and DTNB (2 mM) in Tris-HCl (50 mM, pH 8.0). Absorbance values were recorded every 30 s for 1 h in 96-well plates maintained at 25 °C. To confirm that the Eis_*Mtb* mutants generated did not hydrolyze AcCoA on their own, controls in which AGs were absent were performed for all mutants. No significant cleavage of AcCoA was observed in the absence of AGs.

Determination of the Eis_*Mtb* Mutants Steady-State Kinetic Parameters. Reactions (200 μL) contained a fixed AcCoA concentration (0.5 mM) and AG (KAN, PAR, APR) concentrations of 0, 20, 50, 100, 250, 500, 1000, and 2000 μM. The initiation of reaction mixtures containing DTNB (2 mM), Tris-HCl (50 mM, pH 8.0), and Eis_*Mtb* mutants (0.25 μM for assays with KAN and PAR, 1 μM for assays with APR) was accomplished through the addition of the AG. Assays were performed in triplicate. Absorbance values were recorded at 412 nm every 20 s for 20 min at 25 °C. A nonlinear regression fit to the Michaelis–Menten equation was performed using Sigma Plot 11.0 software (Systat Software Inc., San Jose, CA) to determine the K_m and k_{cat} parameters (Table 1 and Figures S2–S4 of the Supporting Information).

Determination of Degree of Acetylation by Eis_*Mtb* Mutants. Reactions (30 μL) containing PAR (0.67 mM), AcCoA (3.35 mM), Eis enzyme (5 μM), and Tris-HCl (50 mM, pH 8.0) were incubated overnight at rt. Reactions were quenched by the addition of ice-cold methanol (30 μL) and kept at −20 °C for at least 20 min. To remove excess enzyme from the solution, the reaction mixtures were centrifuged (13 000 rpm, 10 min, and rt) and diluted with H_2O (60 μL) prior to loading in the LCMS. The samples were run using H_2O (0.1% formic acid). All mass spectra are presented in Figure S5.

dx.doi.org/10.1021/bi4002985 | *Biochemistry* 2013, 52, 5125–5132

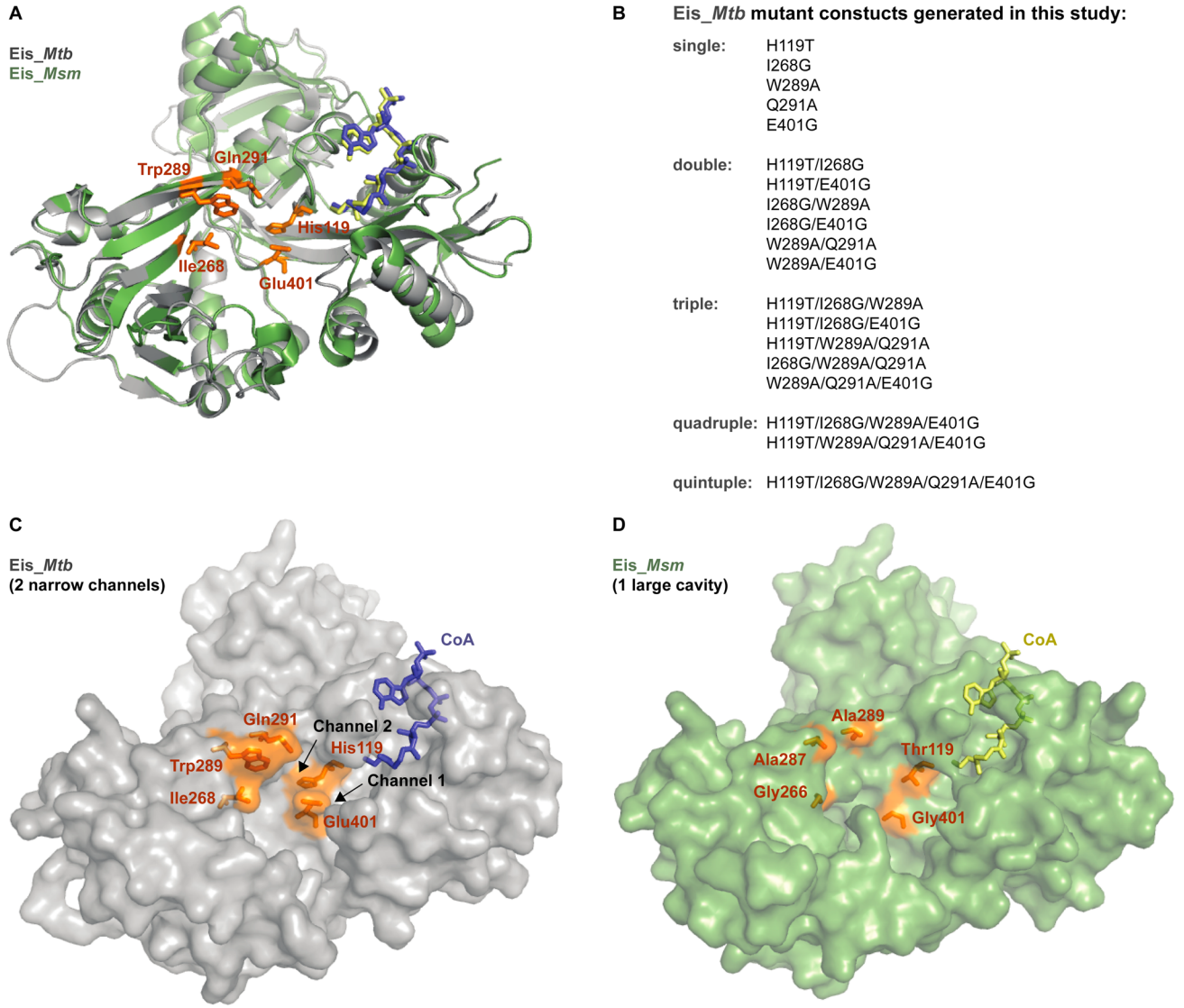

Figure 3. Structural differences between the AG binding pockets of Eis_*Mtb* and Eis_*Msm*. (A) Cartoon overlay of Eis_*Mtb* (gray; PDB code 3R1K[7]) and Eis_*Msm* (green; PDB code 3SXN[11]). Coenzyme A (CoA) is shown as blue (Eis_*Mtb*) or yellow (Eis_*Msm*) sticks. The five residues lining the Eis_*Mtb* AG binding pocket that were mutated in these studies are shown as orange sticks. (B) List of Eis_*Mtb* mutant constructs examined in this study. (C) Surface representation of Eis_*Mtb* (gray) with CoA (blue sticks) and active-site residues (orange sticks). The Eis_*Mtb* active site is divided into two narrow channels by Glu401. (D) Surface representation of Eis_*Msm* (green) with CoA (yellow sticks) and the active-site residues (orange sticks) to which the corresponding Eis_*Mtb* residues were mutated.

Determination of Regiospecificity of Acetylation by TLC. Reactions (30 μL) containing Tris-HCl (50 mM, pH 8.0), Eis enzyme (5 μM), AcCoA (4 mM), and KAN (0.8 mM) were performed at rt. Aliquots (4 μL) were loaded onto a TLC plate (SiO_2 gel 60 F_{254} from Merck) after 0, 1, 5, 10, 30, 120 min, and overnight incubation and run using a 3:1 MeOH/NH_4OH mixture as the eluent system. The plate was dried and visualized by cerium molybdate stain (5 g of CAN, 120 g of ammonium molybdate, 80 mL of H_2SO_4, and 720 mL of H_2O) (Figure S6).

RESULTS

Overexpression and Purification of Eis_*Mtb* Mutants. Recombinant Eis_*Mtb*, Eis_*Msm*, and Eis_*Mtb* mutants were expressed in *E. coli*, purified by Ni^{II}-NTA affinity chromatography (Figure S1 of the Supporting Information), and used in activity assays.

Determination of the Activity of Eis_*Mtb*, Eis_*Msm*, and Eis_*Mtb* Mutants with KAN, PAR, and APR. We first characterized the activity of all Eis_*Mtb* mutants with KAN, PAR, and APR to determine whether they retained acetyltransferase activity. The initial rates of acetylation (CoA release) by the Eis_*Mtb* mutants with KAN, PAR, and APR were calculated. For Eis_*Mtb* mutant−AG combinations with initial rates at or above 10.5 nM/s, we additionally performed Michaelis−Menten analysis of the initial reaction rate as a function of the concentration of AG (Table 1).

Activity of Wild-Type Eis_*Mtb* and Eis_*Msm*. Overall, the initial acetylation rates for Eis_*Msm* with KAN (41 nM/s) and PAR (22 nM/s) were much faster than with APR (2.7 nM/s). Because of the significantly lower activity of Eis_*Msm* with APR and the fact that only Eis_*Mtb*-W289A had detectable activity, the results with APR will be reported later in this section. Relative to that of Eis_*Mtb*, Eis_*Msm* displayed a considerably higher initial rate with PAR and a higher initial

dx.doi.org/10.1021/bi4002985 | *Biochemistry* 2013, 52, 5125−5132

Table 1. Kinetic Parameters for Eis_*Mtb* Mutants with KAN, PAR, and APR

	KAN		
mutant[a]	K_m (μM)	k_{cat} (s^{-1})	k_{cat}/K_m (M^{-1} s^{-1})
Eis_*Mtb*[b]	330 ± 40	0.53 ± 0.03	1606 ± 215
Eis_*Msm*[b]	665 ± 42	0.36 ± 0.01	541 ± 37
H	684 ± 80	0.32 ± 0.02	468 ± 62
I	776 ± 130	0.63 ± 0.05	812 ± 150
W	670 ± 86	0.24 ± 0.01	358 ± 48
Q	438 ± 56	1.08 ± 0.05	2465 ± 335
E	1397 ± 351	0.15 ± 0.02	107 ± 30
HI	813 ± 308	0.06 ± 0.01	74 ± 31
HE	516 ± 139	0.07 ± 0.01	135 ± 41
IW	791 ± 112	0.15 ± 0.01	189 ± 30
IE	908 ± 359	0.11 ± 0.02	121 ± 53
WQ	712 ± 86	0.40 ± 0.02	561 ± 73
WE	679 ± 125	0.13 ± 0.01	191 ± 38
HIW	617 ± 223	0.11 ± 0.02	178 ± 72
HIE	673 ± 203	0.06 ± 0.01	89 ± 31
HWQ	[c]	[c]	[c]
IWQ	620 ± 75	0.37 ± 0.02	597 ± 79
WQE	[c]	[c]	[c]
HIWE	437 ± 96	0.04 ± 0.01	92 ± 30
HWQE	[c]	[c]	[c]
HIWQE	[c]	[c]	[c]
	PAR		
mutant[a]	K_m (μM)	k_{cat} (s^{-1})	k_{cat}/K_m (M^{-1} s^{-1})
Eis_*Mtb*[b]	110 ± 21	0.14 ± 0.01	1272 ± 260
Eis_*Msm*[b]	738 ± 158	0.24 ± 0.03	325 ± 81
H	643 ± 195	0.05 ± 0.01	77 ± 28
I	789 ± 194	0.13 ± 0.01	165 ± 35
W	615 ± 244	0.05 ± 0.01	81 ± 36
Q	1019 ± 358	0.12 ± 0.02	118 ± 46
IW	1005 ± 285	0.07 ± 0.01	70 ± 22
WQ	280 ± 77	0.06 ± 0.01	214 ± 69
WE	486 ± 271	0.04 ± 0.01	82 ± 50
IWQ	452 ± 178	0.05 ± 0.01	111 ± 49
	APR		
mutant[a]	K_m (μM)	k_{cat} (s^{-1})	k_{cat}/K_m (M^{-1} s^{-1})
Eis_*Mtb*	×[d]	×[d]	×[d]
Eis_*Msm*[b]	150 ± 43	0.019 ± 0.002	127 ± 39
W	195 ± 64	0.005 ± 0.001	26 ± 9

[a]The abbreviations for Eis_*Mtb* mutants are based on the amino acid residues of Eis_*Mtb* that were mutated to the corresponding residues from Eis_*Msm*. These abbreviations are used in Figure 4: Eis_*Mtb*-H119T, H; Eis_*Mtb*-I268G, I; Eis_*Mtb*-W289A, W; Eis_*Mtb*-Q291A, Q; and Eis_*Mtb*-E401G, E. [b]These values have been previously reported and are used for comparison in this manuscript.[14] [c]For KAN, kinetic parameters could not be determined for the following mutants because the activity was less than 26% of the initial rate of Eis_*Mtb* with KAN (10.5 nM CoA s^{-1}, Figure 4A): HWQ, WQE, HWQE, and HIWQE. For PAR, kinetic parameters could not be determined for the following mutants because the activity was less than 50% of the initial rate of Eis_*Mtb* with PAR (10.5 nM CoA s^{-1}, Figure 4B): E, HI, HE, IE, HIW, HWQ, WQE, HIWE, HWQE, and HIWQE. For APR, kinetic parameters could be determined only for the W mutant with APR because the activity of all others was too low to be determined (Figure 4C). [d] × indicates that APR is not a substrate of Eis_*Mtb*.

rate with KAN. As previously reported, the K_m values for the AGs are lower for KAN and PAR with wild-type Eis_*Mtb* (K_m = 330 and 110 μM, respectively) than for wild-type Eis_*Msm* with KAN and PAR (K_m = 665 and 738 μM, respectively) (Table 1).[14] The difference in the binding affinities between these two Eis isoforms reflected by these values may result from changes in the AG binding-pocket size and the ability of the residues lining this pocket to interact with the AGs. We tested this hypothesis by analyzing the effects of single and multiple mutations within the AG binding pocket of Eis_*Mtb* (Figure 3).

Activity of Eis_*Mtb* Single Mutants with KAN and PAR. All of the Eis_*Mtb* mutants examined here, in which the residues within Eis_*Mtb* were mutated to those of the corresponding Eis_*Msm* residues, had weaker observed AG binding affinities (higher K_m values) than that of wild-type Eis_*Mtb* ($K_{m,KAN}$ = 330 μM, $K_{m,PAR}$ = 110 μM). The mutations of individual Eis_*Mtb*-to-Eis_*Msm* residues gave mixed results with respect to catalytic efficiencies (Figure 4). Converting His119, Ile268, and Trp289 of Eis_*Mtb* to Thr, Gly, and Ala, respectively, significantly perturbed the catalytic efficiencies of KAN and PAR acetylation. However, mutating Gln291 to Ala resulted in an increase in the reaction efficiency of KAN acetylation but significantly decreased that of PAR acetylation when compared to that of Eis_*Mtb* (Figure 4). The most

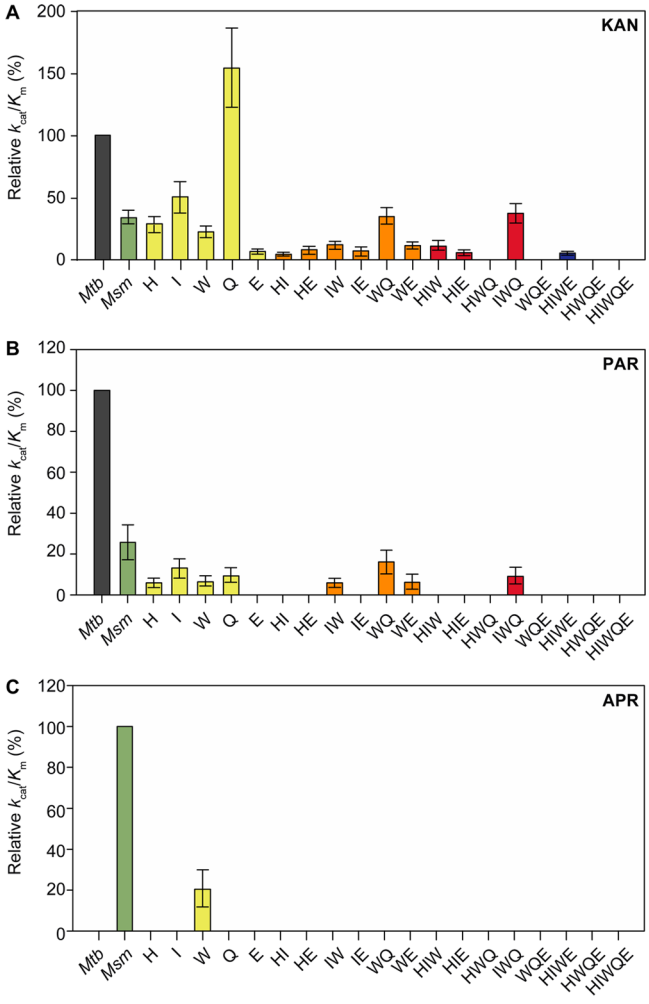

Figure 4. Relative catalytic efficiencies (k_{cat}/K_m) for the Eis_*Mtb* mutants. (A) Activity of the Eis_*Mtb* mutants with KAN (normalized to Eis_*Mtb*-wt (1606 M^{-1} s^{-1})). (B) Activity of Eis_*Mtb* mutants with PAR (normalized to Eis_*Mtb*-wt (1272 M^{-1} s^{-1})). (C) Activity of Eis_*Mtb* mutants with APR (normalized to Eis_*Msm*-wt (127 M^{-1} s^{-1})).

dx.doi.org/10.1021/bi4002985 | *Biochemistry* 2013, 52, 5125−5132

noticeable kinetic difference observed with the single Eis_*Mtb* mutants was the increased k_{cat} of Eis_*Mtb*-Q291A with KAN (k_{cat} = 1.08 s^{-1}), which was 2-fold higher than the catalytic turnover determined for wild-type Eis_*Mtb* with KAN (k_{cat} = 0.53 s^{-1}) and nearly 3-fold higher than that established for wild-type Eis_*Msm* with KAN (k_{cat} = 0.36 s^{-1}). For all single mutants, a decrease in catalytic turnover with PAR was observed, as indicated by a k_{cat} value lower than that for Eis_*Mtb* (k_{cat} = 0.14 s^{-1}). For both KAN and PAR, the Eis_*Mtb*-E401G mutant displayed dramatically reduced activity when compared to that of Eis_*Mtb* (Figure 4), as evidenced by its poor catalytic efficiency for KAN (k_{cat}/K_m = 107 M^{-1} s^{-1}) (Table 1).

Activity of Eis_*Mtb* Multiple Point Mutants with KAN and PAR. Combinations of all mutations resulted in decreased catalytic efficiency with respect to wild-type Eis_*Mtb*, and catalytic efficiencies were even lower than those observed for Eis_*Msm* with the exception of Eis_*Mtb*-W289A/Q291A where the catalytic efficiency of KAN acetylation was roughly equal to that of Eis_*Msm* (Figure 4). Interestingly, triple mutant Eis_*Mtb*-I268G/W289A/Q291A also retained a catalytic efficiency of KAN acetylation equal to that of Eis_*Msm*. In the case of PAR, these two favorable multiple point mutants (W289A/Q291A and I268G/W289A/Q291A) also displayed noticeably higher catalytic efficiencies than any of the other multiple mutants generated, albeit that they were somewhat lower than that of Eis_*Msm*. All multiple point mutants bearing the unfavorable single mutation E401G displayed poor overall activity with KAN and PAR. Aside from these general trends among the mutants studied with KAN and PAR, there were some outlying results observed (e.g., double mutant W289A/E401G displayed catalytic efficiencies superior to those of the single E401G mutant with both KAN and PAR) (Figure 4).

Determination of Degree and Regiospecificity of Acetylation by Eis_*Mtb* Mutants. To establish if the extent of acetylation (mono-, di-, or tri-) of the AG substrates is affected by single-point and multiple-point mutagenesis, we performed mass spectrometric analysis of the enzymatic acetylation of PAR with all of the mutants generated. We found that with the Eis_*Mtb*, Eis_*Msm*, and all Eis_*Mtb* mutants PAR was always triacetylated. Figure S5 displays representative mass spectra of the triacetylation of PAR by Eis_*Mtb*, Eis_*Msm*, Eis_*Mtb*-I268G, Eis_*Mtb*-I268G/W289A, and Eis_*Mtb*-I268G/W289A/Q291A. We also established by TLC time course that mutagenesis did not affect the extent or regiospecificity of the acetylation of KAN, which was always diacetyalted in the same order (Figure S6). All reactions revealed small amounts of monoacetyl-KAN with an identical R_f value of 0.26 in the first minute of the reaction and with the diacetyl-KAN (R_f 0.39) forming within 5 min. All reactions appeared to be complete after 30 min.

Activity of Eis_*Mtb* Mutants with APR. The initial rates of acetylation of APR by Eis_*Mtb* mutants were compared to that of Eis_*Msm* (Figure 4C). Eis_*Msm* acetylates APR much less efficiently than it does KAN or PAR. These measurements are consistent with previously reported k_{cat} values that are an order of magnitude lower for Eis_*Msm* with APR than with KAN or PAR: $k_{cat,KAN}$ = 0.36 s^{-1}, $k_{cat,PAR}$ = 0.24 s^{-1}, and $k_{cat,APR}$ = 0.019 s^{-1}.[14] One single mutant, Eis_*Mtb*-W289A, caused Eis_*Mtb* to behave similarly to Eis_*Msm*: it demonstrated significant APR acetylation activity. The APR acetylation catalytic efficiency of Eis_*Mtb*-W289A was 20% of that of Eis_*Msm*. The binding affinity for APR to Eis_*Mtb*-W289A (K_m = 195 μM) was similar to that of Eis_*Msm* (K_m = 150 μM), whereas the k_{cat} value was 4-fold smaller (0.019 s^{-1} for Eis_*Msm* and 0.005 s^{-1} for Eis_*Mtb*-W289A) (Table 1).

DISCUSSION

Because of its prominent role in bacterial resistance, a better understanding of the activity of the Eis protein is needed. We recently reported the substrate and multiacetylation profiles of Eis_*Mtb* and Eis_*Msm*, demonstrating the unique multiacetylation capabilities of Eis enzymes.[7,9,10] Eis is overall hexameric, featuring tripartite monomers containing N-terminal and central GCN5 *N*-acetyltransferase (GNAT) regions; only the N-terminal GNAT region has catalytic residues (Tyr126 and the C-terminal carboxylate) and binds AcCoA. The overall structures of the Eis proteins from these two mycobacteria are very similar, but the differences include a few important residues in the substrate-binding pockets (Figures 2 and 3). The residues in Eis_*Mtb* tend to be bulkier than those of Eis_*Msm*, leading to differently sized and shaped AG binding pockets (Figure 3); the more open, large cavity of Eis_*Msm* has been proposed to better accommodate larger and/or conformationally constrained AGs.[9]

Redesigning and expanding the substrate-specificity profile of enzymes is a topic of interest for many research groups.[15−20] In this study, we performed site-specific mutational studies for the following reasons: (i) to explore if we could redesign the AG specificity of Eis_*Mtb*, (ii) to understand better which residues of Eis_*Mtb* play an important role in conferring resistance to AGs, (iii) to investigate if we could alter the regiospecificity and/or the number of sites acetylated by Eis_*Mtb* mutants for the future chemoenzymatic formation of novel AGs, and (iv) to gain potential insights into the mechanism of action of Eis enzymes. We mutated five bulky residues that form the AG binding pocket in Eis_*Mtb* to their corresponding smaller residues found in Eis_*Msm*. These mutations are expected to increase the size of the AG binding pocket of Eis_*Mtb* to resemble that of Eis_*Msm* (Figure 3). We chose three AGs for these studies: KAN, PAR, and APR (Figure 1A). KAN was chosen because of its immediate relevance to TB; KAN-resistance in XDR-*Mtb* clinical isolates results from *eis* upregulation.[4] PAR and APR were selected for investigation because they represent additional diverse structural scaffolds; KAN contains a 4,6-substituted 2-deoxystreptamine (4,6-DOS) ring, whereas PAR contains a 4,5-DOS ring with an additional sugar moiety (ring IV). With two of its four rings fused, APR represents a third unique rigid AG scaffold. Additionally, APR is a substrate for Eis_*Msm*, whereas it is a very poor substrate for Eis_*Mtb*.

Effects of Single Mutations on Eis_*Mtb* Activity with KAN and PAR. To gain insight into the role of His119, Ile268, Trp289, Gln291, and Glu401 in Eis_*Mtb* activity and AG binding, we first converted these residues into their corresponding residues found in Eis_*Msm* (Figures 2 and 3). Of the individual mutations of the three residues (I268G, W289A, and Q291A) lining one side of channel 2 in the Eis_*Mtb* AG binding pocket (Figure 3), only Q291A increased catalytic efficiency when compared to that of the wild-type Eis_*Mtb* with KAN. Moreover, Eis_*Mtb*-I268G and Q291A mutants had a higher efficiency with KAN than Eis_*Msm* did. The Q291A mutation led to a dramatic increase in KAN acetylation activity in Eis_*Mtb*, as evidenced by a higher k_{cat} value (1.08 s^{-1}) in comparison to that of Eis_*Msm* (k_{cat} = 0.36 s^{-1}). As hypothesized, the individual I268G and W289A

dx.doi.org/10.1021/bi4002985 | *Biochemistry* 2013, 52, 5125−5132

mutations made Eis_*Mtb* behave more like Eis_*Msm*. Mechanistically, this observed decrease in activity may be explained as follows: a larger cavity may not bind AGs as well as a narrower one, which is consistent with the higher K_m values observed for Eis_*Msm* and Eis_*Mtb* mutants than those for wild-type Eis_*Mtb*.

The Eis_*Mtb*-E401G mutant showed a dramatic decrease in catalytic efficiency with both KAN and PAR when compared to that of either Eis_*Mtb* or Eis_*Msm*. Glu401 is the penultimate residue of the proteins C-terminus and is flanked by C-terminal residue Phe402. The buried side chain of Phe402 points toward the protein interior, positioning the terminal carboxyl group to act as a catalytic base during acetylation. Mutating Glu401 to a flexible Gly may increase the backbone flexibility that is compensated for in the context of the Eis_*Msm* residues but not in those of Eis_*Mtb*, possibly disturbing the position of the terminal carboxyl group. Previous studies found that Eis with a C-terminal His_6 tag or a truncated version (Eis_*Mtb*-1−399) eliminated nearly all acetylation activity, further highlighting the importance of this C-terminal region.[7]

With KAN, Eis_*Mtb*-H119T maintained activity similar to that of Eis_*Msm*. However, with PAR, Eis_*Mtb*-H119T showed a significant decrease in efficiency compared to both wild-type Eis_*Mtb* and Eis_*Msm*. These results in combination with the fact that Eis_*Mtb*-H119A displays very poor activity with KAN and PAR[7] indicate that a polar amino acid residue or a residue that can donate or accept hydrogen bonds may be required at that position in the Eis active site.

Effects of Multiple Mutations on Eis_*Mtb* Activity with KAN and PAR. To determine if the divided Eis_*Mtb* active site could be progressively converted to the larger nondivided Eis_*Msm* AG binding cavity, we next generated a variety of double, triple, quadruple, and quintuple Eis_*Mtb* mutants. The most active double mutant, Eis_*Mtb*-W289A/Q291A, and triple mutant, Eis_*Mtb*-I268G/W289A/Q291A, maintained high activity with KAN equivalent to that of Eis_*Msm*, whereas they displayed a slight decrease in catalytic efficiency with PAR when compared to that of Eis_*Msm* (Figure 4). This agrees well with what was observed with the single mutants, and suggests that the I268G, W289A, and Q291A mutations allow Eis_*Mtb* to become very similar in activity to Eis_*Msm*. All three of these residues line channel 2 of the AG binding site within Eis_*Mtb* (Figure 3). Mutating these residues to smaller side chains enlarges channel 2, which may help to better accommodate both KAN and PAR scaffolds with a decrease in the turnover rate only to the level of Eis_*Msm*. Generally, multiple mutations did not display a consistent additive or nonadditive pattern, which is likely because of their interactions either directly or through the bound AGs. Consistent with the loss of activity for the single Eis_*Mtb*-E401G mutant, all multiple mutants containing the E401G mutation showed a dramatic decrease in activity with KAN and PAR.

Effects of Mutations on Degree and Regiospecificity of Acetylation. To determine the effect of mutating the five residues studied on the degree and regiospecificity of acetylation of KAN and PAR, we performed mass spectrometry and TLC experiments. By mass spectrometry, the single- and multiple-point Eis_*Mtb* mutants did not result in any changes in the number of sites acetylated on PAR (Figure S5). By TLC time course, Eis_*Mtb* mutants were found to acetylate KAN in the same order as that of Eis_*Mtb* and Eis_*Msm* (Figure S6). Monoacetyl-KAN was formed during the first minute of the enzymatic reactions, and diacetyl-KAN was observed after 5 min, with the apparent completion of all diacetylation reactions after 30 min. Identical R_f values for all monoacetyl-KAN (R_f 0.26) and diacetyl-KAN (R_f 0.39) indicated that the mutation of the five residues studied does not alter the regiospecificty of the Eis enzymes.

Effects of Eis_*Mtb* Mutations on Activity with APR. The only mutant that demonstrated detectable activity with the large and rigid APR was Eis_*Mtb*-W289A. This can be easily rationalized by the considerable steric changes that this mutation causes in the AG binding pocket. Trp289 bears a very bulky indole side chain, and eliminating this large group extends the depth of channel 2 in the Eis_*Mtb* active site (Figure 3), making it large enough to accommodate the long restricted structure of APR.

We have presented evidence that three of the five residues mutated, Ile268, Trp289, and Gln291, are important for controlling the efficiency of KAN and PAR acetylation. We have also demonstrated that Trp289 is an important residue for APR acetylation. Finally, we have shown that Glu401 plays a key role in the overall activity of Eis_*Mtb*. It is worth noting that out of the five mutations in this study only the Glu-to-Gly mutation can be achieved by a single nucleotide substitution (and would be inactivating). Therefore, resistance is not likely to evolve further through the mutations that we considered. Our lab is currently investigating Eis inhibitors for use in combination therapy with AGs, and we are examining their effectiveness across a broad spectrum of mycobacterial and nonmycobacterial species containing Eis proteins. In conjunction with our previous work on the identification of inhibitors of Eis_*Mtb*,[21] the knowledge gained in the current study will aid in the design of Eis inhibitors for codelivery with AGs to treat resistant infections.

■ ASSOCIATED CONTENT

Ⓢ Supporting Information

Tables of the primers used in this study, the primer combinations and templates used to construct the Eis_*Mtb* mutants, and the purification yields of the Eis_*Mtb* mutants. SDS-PAGE gel showing all of the Ni^{II}−NTA-purified proteins used in this study, kinetic curves of the Eis_*Mtb* mutants with AGs, representative mass spectra of PAR acetylation by Eis_*Mtb*, Eis_*Msm*, and Eis_*Mtb* mutants, and representative TLC time course of KAN diacetylation by Eis_*Mtb*, Eis_*Msm*, and Eis_*Mtb* mutants. This material is available free of charge via the Internet at http://pubs.acs.org.

■ AUTHOR INFORMATION

Corresponding Author

*E-mail: sylviegtsodikova@uky.edu. Phone: (859) 218-1686. Fax: (859) 257-7585.

Author Contributions

[§]These authors contributed equally to this work.

Funding

Funding support for this work was provided by National Institutes of Health grant AI090048 (to S.G.-T.) and startup funds from the University of Kentucky (to S.G.-T.).

Notes

The authors declare no competing financial interest.

■ ACKNOWLEDGMENTS

We thank Rachel E. Pricer for cloning and preliminary experimental work. We thank Dr. Oleg V. Tsodikov for his critical reading of the manuscript and insightful comments.

■ ABBREVIATIONS

AcCoA, acetyl coenzyme A; AG, aminoglycoside; APR, apramycin; CoA, coenzyme A; DTNB, 5,5′-dithio-(2-nitrobenzoic acid); Eis, enhanced intracellular survival; KAN, kanamycin A; MDR, multidrug-resistant; Msm, *Mycobacterium smegmatis*; Mtb, *Mycobacterium tuberculosis*; PAR, paromomycin; SDS PAGE, sodium dodecyl sulfate polyacrylamide gel electrophoresis; TB, tuberculosis; XDR, extensively drug-resistant

■ REFERENCES

(1) Ellner, J. J. (2008) The emergence of extensively drug-resistant tuberculosis: a global health crisis requiring new interventions: part I: the origins and nature of the problem. *Clin. Transl. Sci. 1*, 249−254.

(2) Banerjee, R., Schecter, G. F., Flood, J., and Porco, T. C. (2008) Extensively drug-resistant tuberculosis: new strains, new challenges. *Expert Rev. Anti-Infect. Ther. 6*, 713−724.

(3) Udwadia, Z. F., Amale, R. A., Ajbani, K. K., and Rodrigues, C. (2012) Totally drug-resistant tuberculosis in India. *Clin. Infect. Dis. 54*, 579−581.

(4) Zaunbrecher, M. A., Sikes, R. D., Jr., Metchock, B., Shinnick, T. M., and Posey, J. E. (2009) Overexpression of the chromosomally encoded aminoglycoside acetyltransferase eis confers kanamycin resistance in Mycobacterium tuberculosis. *Proc. Natl. Acad. Sci. U.S.A. 106*, 20004−20009.

(5) Campbell, P. J., Morlock, G. P., Sikes, R. D., Dalton, T. L., Metchock, B., Starks, A. M., Hooks, D. P., Cowan, L. S., Plikaytis, B. B., and Posey, J. E. (2011) Molecular detection of mutations associated with first- and second-line drug resistance compared with conventional drug susceptibility testing of Mycobacterium tuberculosis. *Antimicrob. Agents Chemother. 55*, 2032−2041.

(6) Jnawali, H. N., Yoo, H., Ryoo, S., Lee, K. J., Kim, B. J., Koh, W. J., Kim, C. K., Kim, H. J., and Park, Y. K. (2013) Molecular genetics of Mycobacterium tuberculosis resistant to aminoglycosides and cyclic peptide capreomycin antibiotics in Korea. *World J. Microbiol. Biotechnol. 29*, 975−982.

(7) Chen, W., Biswas, T., Porter, V. R., Tsodikov, O. V., and Garneau-Tsodikova, S. (2011) Unusual regioversatility of acetyltransferase Eis, a cause of drug resistance in XDR-TB. *Proc. Natl. Acad. Sci. U.S.A. 108*, 9804−9808.

(8) Reyrat, J. M., and Kahn, D. (2001) Mycobacterium smegmatis: an absurd model for tuberculosis? *Trends Microbiol. 9*, 472−474.

(9) Chen, W., Green, K. D., Tsodikov, O. V., and Garneau-Tsodikova, S. (2012) Aminoglycoside multiacetylating activity of the enhanced intracellular survival protein from Mycobacterium smegmatis and its inhibition. *Biochemistry 51*, 4959−4967.

(10) Houghton, J. L., Green, K. D., Pricer, R. E., Mayhoub, A. S., and Garneau-Tsodikova, S. (2012) Unexpected N-acetylation of capreomycin by mycobacterial Eis enzymes. *J. Antimicrob. Chemother. 68*, 800−805.

(11) Kim, K. H., An, D. R., Song, J., Yoon, J. Y., Kim, H. S., Yoon, H. J., Im, H. N., Kim, J., Kim do, J., Lee, S. J., Lee, H. M., Kim, H. J., Jo, E. K., Lee, J. Y., and Suh, S. W. (2012) Mycobacterium tuberculosis Eis protein initiates suppression of host immune responses by acetylation of DUSP16/MKP-7. *Proc. Natl. Acad. Sci. U.S.A. 109*, 7729−7734.

(12) Ho, S. N., Hunt, H. D., Horton, R. M., Pullen, J. K., and Pease, L. R. (1989) Site-directed mutagenesis by overlap extension using the polymerase chain reaction. *Gene 77*, 51−59.

(13) Riddles, P. W., Blakeley, R. L., and Zerner, B. (1983) Reassessment of Ellman's reagent. *Methods Enzymol. 91*, 49−60.

(14) Pricer, R. E., Houghton, J. L., Green, K. D., Mayhoub, A. S., and Garneau-Tsodikova, S. (2012) Biochemical and structural analysis of aminoglycoside acetyltransferase Eis from Anabaena variabilis. *Mol. BioSyst. 8*, 3305−3313.

(15) Green, K. D., Porter, V. R., Zhang, Y., and Garneau-Tsodikova, S. (2010) Redesign of cosubstrate specificity and identification of important residues for substrate binding to hChAT. *Biochemistry 49*, 6219−6227.

(16) Williams, G. J., Zhang, C., and Thorson, J. S. (2007) Expanding the promiscuity of a natural-product glycosyltransferase by directed evolution. *Nat. Chem. Biol. 3*, 657−662.

(17) Moretti, R., Chang, A., Peltier-Pain, P., Bingman, C. A., Phillips, G. N., Jr., and Thorson, J. S. (2011) Expanding the nucleotide and sugar 1-phosphate promiscuity of nucleotidyltransferase RmlA via directed evolution. *J. Biol. Chem. 286*, 13235−13243.

(18) Yi, H., Cho, K. H., Cho, Y. S., Kim, K., Nierman, W. C., and Kim, H. S. (2012) Twelve positions in a beta-lactamase that can expand its substrate spectrum with a single amino acid substitution. *PLoS One 7*, e37585-1−e37585-11.

(19) Rale, M., Schneider, S., Sprenger, G. A., Samland, A. K., and Fessner, W. D. (2011) Broadening deoxysugar glycodiversity: natural and engineered transaldolases unlock a complementary substrate space. *Chem.—Eur. J. 17*, 2623−2632.

(20) Addington, T., Calisto, B., Alfonso-Prieto, M., Rovira, C., Fita, I., and Planas, A. (2011) Re-engineering specificity in 1,3-1, 4-beta-glucanase to accept branched xyloglucan substrates. *Proteins 79*, 365−375.

(21) Green, K. D., Chen, W., and Garneau-Tsodikova, S. (2012) Identification and characterization of inhibitors of the aminoglycoside resistance acetyltransferase Eis from Mycobacterium tuberculosis. *ChemMedChem 7*, 73−77.